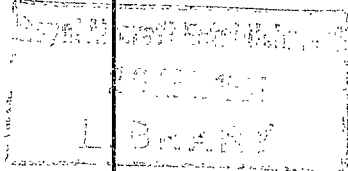




MINISTRY OF SUPPLY

AERONAUTICAL RESEARCH COUNCIL
REPORTS AND MEMORANDA



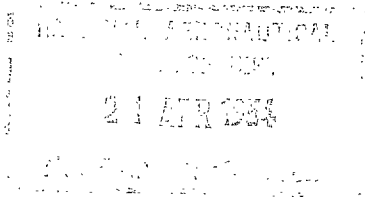
The Flutter of Swept and Unswept Wings with Fixed-Root Conditions

PART I—Wind-Tunnel Experiments
PART II—Comparison of Experiment and Theory
PART III—Wing Torsional Stiffness Criterion

By

W. G. MOLYNEUX, B.Sc.

Crown Copyright Reserved



LONDON: HER MAJESTY'S STATIONERY OFFICE

1954

PRICE 6s 6d NET

The Flutter of Swept and Unswept Wings with Fixed-Root Conditions

Parts I, II and III

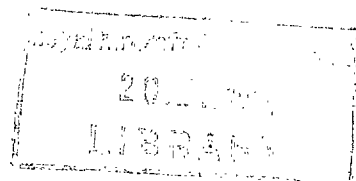
By

W. G. MOLYNEUX, B.Sc.

COMMUNICATED BY THE PRINCIPAL DIRECTOR OF SCIENTIFIC RESEARCH (AIR),
MINISTRY OF SUPPLY

*Reports and Memoranda No. 2796**

January, 1950



Summary.—The 'fixed-root' flexure-torsion flutter characteristics of four model wings of different taper ratios have been investigated in the wind tunnel. The wing inertia axis and the angle of sweepback have been varied on each wing over the ranges 0.4c to 0.5c and 0 deg to 50 deg respectively. The results show that :—

- (i) The flutter speed at any angle of sweepback (including the unswept case) varies approximately linearly with inertia axis position increasing as the inertia axis is moved forward and approximately linearly with wing taper ratio increasing as the taper is increased.
- (ii) The flutter speed decreases slightly for small angles of sweepback and then increases rapidly as sweepback increases.

The results of one theoretical treatment gave good agreement with experiment for variation of flutter speed with sweepback and inertia axis.

The experimental results support the present wing torsional stiffness criterion. Simple amendment to the criterion are put forward for the effects of sweepback.

1.—*General Introduction.*—Wind-tunnel experiments (R. & M. 2626¹) and theoretical investigations² have shown that body freedoms (*i.e.*, the freedoms of the whole aircraft as a rigid body) play an important part in the flutter of aircraft with swept-back wings but that 'fixed root' flutter is likely to occur in some conditions. Part I of the present report describes wind-tunnel fixed-root flutter tests on four straight tapered model wings of equal aspect ratio and mean chord but having different taper ratios. The inertia axis of each wing was variable and the wing could be swept back by rotation about an axis perpendicular to the wing in the plane of the root section. The effects of inertia axis, taper ratio and sweepback variation could thus be investigated. The results show that for fixed-root flutter beneficial effects are obtained from a forward inertia axis, high wing-taper in plan form and medium-high sweepback. A comparison of the experimental results with those from a theoretical treatment by Minhinnick gives good agreement (Part II). A simple approximation for the effect of sweepback is suggested for use with the existing criterion (R. & M. 2154³) for flutter prevention (Part III).

A comparison of fixed-root and body-freedom flutter is obviously a valuable step in comparing theory and experiment and experiments are accordingly proceeding on two wings of this series with body freedoms. The results will form the subject of a separate report.

* R.A.E. Rept. Structures 58, received 18th August, 1950.

PART I

Wind-Tunnel Experiments on Swept and Unswept Wings

1.1. *Introduction.*—The experiments were made in the Royal Aircraft Establishment 5 ft Wind Tunnel and are thereby limited to low speed, but since the main object of the work is to determine the effect of elastic and inertia parameters and the direct effects of the aerodynamic forces due to sweepback this limitation is not considered serious. The high-speed aerodynamic effects on swept-back wings is the subject of separate investigations using the dropped body and ground-launched rocket techniques.

1.2. *Details of the Model Wings.*—Four wings were constructed of taper (tip chord to root chord) 1 : 1, 3 : 4, 1 : 2 and 1 : 4 respectively.

The main structural component of the wings was a square-sectioned spruce spar, tapered in width and depth in the same way as the overall wing taper. This spar carried uniformly spaced wooden ribs of symmetrical section fixed perpendicular to the spar. The spar was situated at 35 per cent of the wing chord. A paper nose-cap and a very light trailing-edge member were fitted to each wing so as to make a negligible contribution to the wing stiffness. The wing covering was of fine silk doped with a solution of vaseline in chloroform to produce a non-porous and flexible skin.

This form of construction was chosen in order to concentrate the main stiffness of the wings in the spar and it was checked experimentally that the wing flexural axis lay along the spar.

Each wing rib contained lead weights screwed into pockets on the aerofoil surface (Fig. 1) and accessible without disturbing the wing covering. By a positioning of these weights three separate locations of the wing inertia axis could be obtained at $0.40c$, $0.45c$ and $0.50c$.

The complete wing was mounted in a solid ash-root block (Fig. 1) which had high flexural and torsional rigidity compared with that of the wing itself.

The wings were originally intended for flutter tests of unswept wings for comparisons with the theoretical work of Collar, Broadbent and Puttick (R. & M. 2154³) and were subsequently modified for the investigation of sweepback. The main modification was alteration of the tips of all the wings so that for a sweepback angle of 35 deg (the mean angle for the range of sweepback considered) the tip rib was parallel to the airstream. The spar length from root to tip was unaltered. This modification caused the wing inertia axis to curve aft at the wing tip, in contrast to the straight inertia axis at a fixed fraction of the chord for the unmodified wing. The most marked change in mass distribution was obtained for the wing with the greatest tip chord, *i.e.*, the untapered wing, the effect decreasing as the tip chord decreased.

The root block for the swept-back wings was also a modification of that used for the unswept case and stiffness tests were made to form an estimate of its effect. It was found that the torsional stiffness of the wing was not measurably affected and the flexural stiffness was slightly decreased.

The effect of a slight change of flexural stiffness on the flutter of an unswept wing is known to be negligible.

Further details of the wings including dimensions, mass and inertia distributions are given in Tables 1 and 2. The effects of temperature and humidity on the wooden structure of the wings was found to be negligible as regular check measurements indicated flutter speed changes of less than 2 per cent over a period of three months. This repeatability of flutter speed was particularly marked on the wing of taper ratio 1 : 2 which, in a further series of tests, was fluttered on more than seventy occasions. There was, however, a sharp change in flutter speed on all the wings when first fluttered, as described in section 1.3.1, and this is attributed to 'settling down' of the wing structure.

1.3. *Measurement of the Wing Elastic and Inertia Characteristics.*—1.3.1. *Stiffness Tests.*—Load was applied to the wing through a contour frame fitted to a wing rib at a section approximately 70 per cent of the span from the wing root, and deflections were measured at this section and at the root by dial gauges.

Wing torsional stiffness was determined from deflection measurements with a pure torque applied about the wing flexural axis, and flexural stiffness from deflection measurements with a concentrated load applied at the wing flexural axis. The root dials served to check the rigidity of the root block. No corrections for root movement were made to the stiffness values, which are given in Table 3, since the overall stiffness (between 0.7 section and centre-line) was considered relevant to the flutter characteristics.

Measurements of wing torsional stiffness were made after each series of flutter tests to indicate changes in the characteristics of the wings. After the first occasion on which the wing was fluttered the torsional stiffness fell sharply and a total of some ten minutes of flutter oscillations was required before a stable value of stiffness was achieved. For the untapered wing this effect was particularly pronounced and a fall in stiffness of about 40 per cent was obtained. However, measurements of flutter characteristics were not made until the torsional stiffness had reached a fairly stable value. It should be mentioned that the stiffness measurements were themselves subject to possible experimental error of ± 3 to 4 per cent. The stiffness values given in Table 3 show a general tendency for a decrease in torsional stiffness and an increase in flexural stiffness with increasing wing taper. However, the wing of taper ratio 3 : 4 does not follow the general trend and this can only be attributed to lower values of flexural and torsional rigidity for the spruce spar. The material for the spars was not specifically selected for uniformity of grain structure and density.

1.3.2. *Resonance Tests.*—The flutter rig (described in section 4.1) was used as a mounting for the wing for the resonance tests, to give the same conditions of root constraint as applied during the flutter tests.

The first three normal modes for each wing for the most-aft position of the wing inertia axis are shown in Figs. 2 to 5. The modes for the wings of taper ratios 1 : 1, 3 : 4 and 1 : 2 are similar in character, whilst the modes for the wing of taper ratio 1 : 4 differ due to the reversed order of the frequencies of the overtone flexure mode and the fundamental torsion mode as compared with the other wings. The effect of change of wing inertia axis position upon the wing resonance frequencies is shown in Table 3. In general a rearward movement of the inertia axis leads to a decrease in the frequencies of the first three resonance modes and the interval of frequency between successive resonances is reduced. This reduction of frequency interval is not apparent on the wing of taper ratio 1 : 4 and is probably due to the proximity of the frequencies of the second and third resonances. These frequencies are almost coincident when the wing inertia axis, g , is at $0.4c$. The variation in nodal line location of the predominantly torsional resonance with variation of inertia axis position is shown in Fig. 6. To a first approximation rearward movement of the inertia axis produces a rearward rotation of the wing nodal line about the wing root. The nodal lines were not obtained on the 1 : 4 wing due to the frequency proximity previously mentioned and the line shown for $g = 0.5c$ was not a true nodal line but was a line of minimum wing amplitude.

During the tests on the wing of taper ratio 3 : 4 a resonance of the wing in yaw occurred at a frequency of about 8 c.p.s. No measurements of the mode were made. This resonance is of interest since it provides an explanation for peculiarities in the flutter characteristics of this wing (see section 1.4.2).

1.4. *Flutter Tests.*—1.4.1. *Description of the Flutter Rig.*—The rig (Fig. 1) comprised a light but rigid braced structure supporting a pivoted platform upon which the wing was mounted in a vertical attitude and to which were attached the arms carrying the flutter safety grab. A fairing was fitted to ensure a smooth airflow over the wing.

The flutter grab was provided to guard against destruction of the wing in a divergent flutter. It consisted of two pincer arms controlled by a hand-operated tension wire to grip the wing on the spar axis at a section about 70 per cent of the wing span from the root.

The angle of wing sweepback was varied by rotating the platform about an axis through the wing trailing edge at the root, and angles of sweepback of the wing spar of 20 deg, 30 deg, 35 deg, 40 deg and 50 deg could be obtained.

1.4.2. *Test Procedure.*—The flutter tests were made in the R.A.E. 5-ft diameter Open Jet Wind Tunnel. The tunnel was found to be suitable for flutter tests since the model was accessible and a simple means for initiation of the flutter could be used. The tests on all the wings were conducted at zero wing incidence.

To initiate flutter the tunnel-wind speed was increased by small increments, whilst continually disturbing the airflow, until a critical speed was reached at which the wing developed self-maintained oscillations. The airflow was disturbed upstream from the model to set the model oscillating, and the approach of flutter was indicated by a slow rate of decay of the wing oscillations. When a disturbance was not used the critical flutter speed could be considerably exceeded and when wing oscillations occurred they were violent necessitating immediate use of the grab. With agitation the wings were found to be sensitive to speed changes of less than 0.5 per cent and in most cases it was found possible to obtain a fairly stable condition with a wing-tip amplitude of about ± 1 in.

The flutter frequency was determined by a stroboscope, which also provided a means of observing the character of the flutter. However, only visual observations of the flutter characteristics were made and actual measurements of the amplitude and phase angles of the flutter mode were not attempted. These observations were found to be of value in indicating a difference in the flutter characteristics of the wing of taper ratio 3 : 4 as compared with those of the other wings. In general, observations of the wing tip demonstrated that the flutter was flexure-torsion in character, but for the 3 : 4 wing the flexure-torsion oscillations were associated with considerable oscillation of the wing in yaw. This was undoubtedly due to the proximity of the natural yawing frequency of the wing to the flutter frequency and may provide an explanation for the peculiarities in the flutter curves for this wing as compared with those for the remainder of the wings.

1.5. *Discussion of Results.*—The experimental results for all the wings are plotted in Figs. 7 to 10.

1.5.1. *The Effect of Change in Inertia Axis Position.*—This effect is shown in Figs. 7 and 8 in which flutter speed is plotted against inertia axis position at three different angles of wing sweepback (0 deg, 35 deg, 50 deg) for each wing. The experimental points are compared with the theoretical form of variation of flutter speed with inertia axis position suggested by the criterion of Ref. 3, namely that V is inversely proportion to $(g - 0.1)$. In general the experimental variation is more nearly linear than is suggested by the criterion relationship but the agreement is otherwise quite reasonable. It is apparent from Figs. 7 and 8 that the rate of change of flutter speed with inertia axis position is influenced by the angle of wing sweepback, being greatest at 0 deg sweepback and decreasing as the angle of sweepback increases. The wing of taper ratio 1 : 4 differs from the other wings in the degree of agreement between experiment and the criterion. For this wing the best agreement is obtained at a sweepback of 50 deg, whereas the results for the 1 : 1, 3 : 4 and 1 : 2 wings agree most closely with the criterion curves at 0 deg sweepback, *i.e.*, for the 1 : 4 wing the rate of change of flutter speed with sweepback is increased as compared with the other wings, and this may be due to the high wing-taper.

An increase of flutter frequency of approximately 10 per cent was obtained with rearward movement of the inertia axis. An approximate average value of flutter frequency has been quoted for each wing in Figs. 9 and 10.

A further effect of inertia axis variation was in the decreasing stability of the flutter with forward movement of the inertia axis. In general the flutter was stable over a small range of wind speed, increasing speed merely resulting in an increase of the amplitude of flutter, but the effect of forward movement of the inertia axis was to reduce this speed range so that small changes in tunnel speed were more likely to produce a divergent oscillation.

1.5.2. *The Effect of Wing Taper Ratio.*—The effect of taper is difficult to assess for whereas the inertia axis effect can be assessed by considering each wing separately, with confidence that other parameters affecting flutter speed will remain constant, for the taper effect all four wings must be considered together, and other parameters than taper ratio vary from wing to wing. Apart from the variation in wing taper ratio the wing-to-wing variations most influencing flutter speed are the variation of wing torsional stiffness, m_0 , and the variation of wing stiffness ratio, r . To derive the taper effect a form of variation of flutter speed, V , with m_0 and r must be presupposed, and the form proposed in the criterion of Ref. 3 is adopted here.

V was first assumed proportional to $m_0^{1/2}$ and the experimental values of flutter speed for all the wings corrected to the value of m_0 for the 1 : 1 wing. The corrected values of V are plotted against $(1 - k)$, (where k is the taper ratio), in Figs. 11 and 12, and are compared with the theoretical form of variation suggested in Ref. 3, namely that V is proportional to $(1 - 0.8k + 0.4k^2)$. The best agreement is obtained at 0 deg sweepback, but even in this case there is a marked deviation due to falling-off of the experimental rate of increase of flutter speed for high wing-taper. The degree of agreement of theory and experiment for wing sweepbacks of 20 deg, 35 deg and 50 deg is poor. As a further step the experimental values of V were corrected to the values of m_0 and r for the 1 : 1 wing by assuming V proportional to $m_0^{1/2}(1 - 0.1r)$, and this result is plotted in Figs. 13 and 14 and compared with the theoretical variation. In general the agreement of the corrected experimental values with the theoretical curves is poor. The experimental results indicate an approximately linear increase of flutter speed with taper and a variation of the form V proportional to $(0.9 - 0.33k)$ is seen to give more reasonable agreement than is obtained with the theoretical curve. However, it can be seen from Figs. 13 and 14 that the experimental rate of increase of flutter speed with taper ratio is affected to some extent by wing inertia axis position and by wing sweepback, increasing with forward movement of the inertia axis and increasing as the angle of sweepback increases, and the suggested linear variation of flutter speed with taper ignores these effects.

1.5.3. *The Effect of Angle of Sweepback.*—The curves of flutter speed against angle of sweepback are given in Figs. 9 and 10. It should be noted that angle of sweepback is the sweepback of the wing main spar at 35 per cent of the chord. In plotting the experimental points the speeds obtained at zero sweepback on the unmodified wings have been associated with the speeds obtained at the various sweepback angles on the modified wings and all points joined by a continuous curve. On this basis there is, in general, a tendency for the flutter speed to decrease with small sweepback angle, reaching a minimum value at a sweepback of about 10 deg and then to increase quite rapidly as the sweepback increases. It is difficult to assess the contribution of the tip modification to this effect but the contribution will decrease with taper. This effect of sweepback is reproduced in the theoretical curves of Fig. 15 (*see* Part II) using a method proposed by Minhinnick and is also obtained by Jordan using a different theoretical approach.

The flutter frequency was found to be comparatively insensitive to angle of sweepback but increased slightly with increasing sweepback.

1.6. *Conclusions.*—It should be noted that the following conclusions are for ‘fixed-root’ flutter of wings which are swept back by rotation about the root.

(a) The flutter speed first tends to decrease slightly, for small angles of sweepback, then increases rapidly as the angle of sweepback increases.

(b) At any given angle of sweepback the flutter speed varies approximately linearly with inertia axis position, increasing with forward movement of the inertia axis.

(c) At any given angle of sweepback the flutter speed varies approximately linearly with taper, increasing as the taper increases.

(d) The rate of change of flutter speed with inertia axis position increases with decreasing angle of sweepback and with increasing wing taper.

(e) The rate of change of flutter speed with wing taper increases with increasing angle of sweepback and with forward movement of the wing inertial axis.

(f) The flutter frequency increases with rearward movement of the wing inertia axis and with increase in the angle of sweepback.

1.7. *Further Developments.*—(a) Flutter experiments are in hand on two wings of this series with body freedoms in pitch and vertical translation, and modifications to the test rig to include freedom in roll are under consideration.

(b) Measurement of the flutter mode for fixed root and body freedom cases is in hand.

(c) Further wind-tunnel experiments are contemplated to investigate the effect of concentrated masses on the wings representing engines and external stores.

(d) The effect of high speed on the flutter of swept wings is being investigated using the flight techniques of dropped bodies and ground-launched rockets.

TABLE 1

Wing Details

Except where otherwise stated the details given below refer to the wing before modifications to the tip.

Span (root to tip along spar),	$s = 4 \text{ ft}$
Mean chord perpendicular to spar	$c_m = 1 \text{ ft}$
Rib spacing	$= 1 \text{ in.}$
Wing spar location as a fraction of the wing chord aft of leading edge, h	$= 0.35c$
Wing mass per unit span	$\sigma c^2 = 1.2c^2 \text{ lb/ft}$

TABLE 2

Variation of Section Radius of Gyration with Inertia Axis Position

Inertia axis location as a fraction of the chord aft of leading edge g	Sectional radius of gyration about the inertia axis as a fraction of the wing chord k_g
0.40c	0.179c
0.45c	0.209c
0.50c	0.235c

TABLE 3

Wing Stiffnesses and Natural Frequencies

Wing taper ratio k Tip chord Root chord	Torsional stiffness at 70 per cent span lb ft/radn m_θ	Flexural stiffness at 70 per cent span lb ft/radn I_ϕ	Inertia axis Location g	Resonance frequencies (these frequencies are for the wing with modified tip) n		
				First	Second	Third
1 : 1	27.8	417	0.40	3.6 flexure	14.9 torsion	23.3 flexure
			0.45	3.6 "	14.5 "	22.6 "
			0.50	3.5 "	13.9 "	21.6 "
3 : 4	19.8	454	0.40	3.6 "	13.4 "	18.8 "
			0.45	3.5 "	13.0 "	18.6 "
			0.50	3.4 "	12.5 "	18.2 "
1 : 2	21.7	582	0.40	5.0 "	16.0 "	20.2 "
			0.45	4.9 "	15.6 "	19.8 "
			0.50	4.7 "	14.8 "	18.8 "
1 : 4	20.0	648	0.40	6.4 "	19.7 "	19.8 "
			0.45	6.0 "	18.4 flexure	18.5 torsion
			0.50	5.8 "	15.0 "	16.4 "

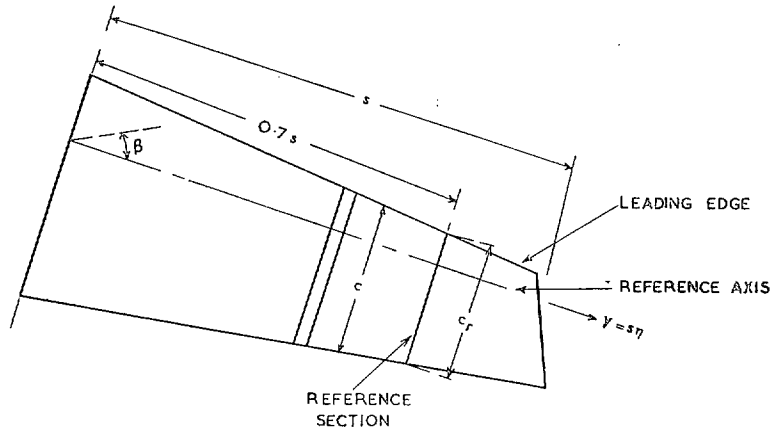
PART II

Comparison of Experiment and Theory

2.1. *Introduction.*—A theoretical investigation on the effect of angle of sweepback and inertia axis position upon flutter speed has been made for the wing of taper ratio 1 : 2. The results have been compared with the experimental values of Part I and show good agreement in the characteristics of the variation of flutter speed with sweepback and inertia axis position.

2.2. *Theoretical Treatment.*—The formulation of the flutter equation is outlined below and is based on the work of Minhinnick. The method is based on the two-dimensional theory for a swept-back wing, in which the forces on elemental strips perpendicular to the wing flexural axis are considered. Since the wing construction was such that sections perpendicular to the flexural axis remained rigid this was thought to be the most suitable method to adopt.

The calculation was made in only two degrees of freedom, namely the first two wing-normal modes, and on the basis of calculations on fixed-root unswept wings it was considered that this would give the flutter speed to an acceptable degree of accuracy. The normal modes chosen were the first and second resonance modes as obtained with the wing inertia axis at 50 per cent chord (*see* Fig. 4). It was decided to ignore the added complication of variation of mode; theoretical investigations on unswept wings have shown that mode variation of the order which occurred on these wings is not likely to be significant.



Let $sf_i(\eta)$ represent the downward displacement of the wing reference axis in mode q_i and let $\frac{s}{c_r} F_i(\eta)$ represent the nose-up twist about the wing reference axis in mode q_i .

Then the downward displacement of the reference axis may be written

$$z = s(f_1q_1 + f_2q_2 + \dots)$$

and the nose-up twist about this axis may be written

$$\alpha = \frac{s}{c_r} (F_1q_1 + F_2q_2 + \dots)$$

The derivatives l_z, l_x, l_y , etc., are evaluated for the reference axis and new derivatives determined from the equations

$$l_b = l_z - \frac{l_x}{\omega^2}, \quad l_t = l_x - l_b, \quad l_i = l_x + \frac{l_z - l_x}{\omega^2}$$

$$m_b = m_z - \frac{m_x}{\omega^2}, \quad m_t = m_x - m_b, \quad m_i = m_x + \frac{m_z - m_x}{\omega^2}$$

all the derivatives will vary along the span of the wing but it is assumed in practice that the values for the reference section apply to the whole wing.

Let
$$K = \frac{c_r}{s} \tan \beta .$$

Then the aerodynamic coefficients in the equations of motion are given in non-dimensional form by the equations

Inertia

$$\begin{aligned} \bar{a}_{ij} = \int & \left[\left(\frac{c}{c_r} \right) l_z f_i f_j + \left(\frac{c}{c_r} \right)^3 (l_\alpha - h l_z) f_i F_j \right. \\ & \left. - \left(\frac{c}{c_r} \right)^3 (m_z + h l_z) f_j F_i - \left(\frac{c}{c_r} \right)^4 \{ m_\alpha + h(l_\alpha - m_z) - h^2 l_z \} F_i F_j \right] d\eta . \end{aligned}$$

Damping

$$\begin{aligned} b_{ij} = \int & \left[\left(\frac{c}{c_r} \right) l_z f_i f_j + \left(\frac{c}{c_r} \right)^2 (l_\alpha - h l_z) f_i F_j - \left(\frac{c}{c_r} \right)^2 (m_z + h l_z) f_j F_i \right. \\ & \left. - \left(\frac{c}{c_r} \right)^3 \{ m_\alpha + h(l_\alpha - m_z) - h^2 l_z \} F_i F_j \right. \\ & \left. + K \left\{ \left(\frac{c}{c_r} \right)^2 l_b f_i f_j' + \left(\frac{c}{c_r} \right)^3 (l_i - h l_b) f_i F_j' - \left(\frac{c}{c_r} \right)^3 (m_b + h l_b) F_i f_j' \right. \right. \\ & \left. \left. - \left(\frac{c}{c_r} \right)^4 \{ m_i + h(l_i - m_b) - h^2 l_b \} F_i F_j' \right\} \right] d\eta . \end{aligned}$$

Stiffness

$$\begin{aligned} c_{ij} = \int & \left[l_x f_i f_j + \left(\frac{c}{c_r} \right) (l_\alpha - h l_z) f_i F_j - \left(\frac{c}{c_r} \right) (m_z + h l_z) f_j F_i \right. \\ & \left. - \left(\frac{c}{c_r} \right)^2 \{ m_\alpha + h(l_\alpha - m_z) - h^2 l_z \} F_i F_j \right. \\ & \left. + K \left\{ \left(\frac{c}{c_r} \right) l_x f_i f_j' + \left(\frac{c}{c_r} \right)^2 (l_i - h l_z) f_i F_j' - \left(\frac{c}{c_r} \right)^2 (m_z + h l_z) F_i f_j' \right. \right. \\ & \left. \left. - \left(\frac{c}{c_r} \right)^3 \{ m_i + h(l_i - m_z) - h^2 l_z \} F_i F_j' \right\} \right] d\eta \end{aligned}$$

where h = distance of reference axis aft of leading edge expressed as a fraction of the chord.

The structural inertia terms are given by

$$\hat{a}_{ij} = \frac{1}{\rho c_r^2} \int m \left\{ f_i f_j + \frac{\bar{x}}{c_r} (F_i f_j + f_i F_j) + \frac{k^2}{c_r^2} F_i F_j \right\} d\eta$$

where

- m is mass of wing/unit length along spar
- \bar{x} co-ordinate of c.g. of section
- k radius of gyration of section about reference axis
- ρ air density.

Since the resonance test (still air) modes are used

$$\hat{a}_{ij} + \bar{a}_{ij} = 0 \text{ for } i \neq j.$$

The equations of motion then assume the form

$$[-a\omega^2 + ib\omega + c + ey]q = 0 \quad \dots \quad (1)$$

where

$$\omega \text{ is frequency parameter} = \frac{c_r \phi}{V \cos \beta}$$

ϕ is flutter frequency in radians per sec

$$a = [a_{ij}] = [\bar{a}_{ij} + \hat{a}_{ij}]$$

and

$$e_{ii}y = \frac{c_r^2}{V^2 \cos^2 \beta} a_{ii} 4\pi^2 n_i^2$$

where

n_i = frequency of i th normal mode in cycles per second. It is convenient to write $e_{ii} = 1$, so that

$$y = \frac{4\pi^2 c_r^2 a_{ii} n_i^2}{V^2 \cos^2 \beta}$$

$$e_{jj} = \frac{a_{jj} n_j^2}{a_{ii} n_i^2}.$$

Equations (1) are then solved for flutter speed and frequency parameter.

2.3. Comparison of Experiment and Theory.—The experimental and theoretical curves of flutter speed against sweepback are shown in Fig. 15. The curves have similar characteristics in the variation of flutter speed with sweepback, flutter speed falling to a minimum at a sweepback of about 10 deg, and in the linearity of the variation of flutter speed with inertia axis position (Fig. 8 wing taper 1 : 2). Also it can be seen from Fig. 8 that the rate of change of flutter speed with inertia axis position agrees with the experimental result in that it increases with decreasing sweepback. However, the theoretical flutter speeds are in all cases lower than those obtained experimentally, which is to be expected since no corrections for the effect of aspect ratio were made to the aerodynamic derivatives (aerodynamics of steady motion⁵ suggests that two-dimensional coefficients are modified by the factor $A/(2 + A)$, where A is the aspect ratio, and a similar modification is probably required on the oscillatory coefficients).

2.4. Conclusions.—The characteristics of the curves of flutter speed against sweepback and inertia axis given by Minhinnick's theory are similar to those obtained experimentally and the agreement between the practical and theoretical values of flutter speed compares favourably with that obtained in the equivalent two-dimensional treatment of an unswept wing.

PART III

Wing Torsional Stiffness Criterion

3.1. *Introduction.*—The present form of the wing torsional stiffness criterion (R. & M. 2154³) for unswept wings is given in the form:—

$$\frac{1}{V} \left(\frac{m_0}{\rho_0 \bar{d} c_m^2} \right)^{1/2} = 0.9 \frac{(g - 0.1)(1.3 - h)}{(1 - 0.8k + 0.4k^2)(1 - 0.1r)} \quad \dots \quad \dots \quad \dots \quad \dots \quad (1)$$

and one object of the experiments of Part I of this report was to investigate the dependence of the flutter speed (V) on the wing inertia axis position (g) and wing taper ratio in planform (k), for comparison with the form of the variation given above which has been obtained on a theoretical basis³.

The extension of the experiments to cover swept-back wings provides experimental data on which an extension of the criterion to sweepback can be based.

3.2. *Criterion for the Unswept Wing.*—3.2.1. *Flutter Speed as a Function of Inertia Axis Location.*—The values of critical speed for different inertia axis locations of the unswept wings are plotted in Figs. 7 and 8 and are compared with the criterion variation of V inversely proportional to $(g - 0.1)$. The experimental variation is more linear than the criterion suggests but the agreement between the experimental points and the curve of V inversely proportional to $(g - 0.1)$ is quite good except for the most highly tapered wing. The disagreement in the latter case is due to the increased rate of change of flutter speed with inertia axis position which is obtained on this wing. However, the maximum deviation between experiment and the criterion is only about 10 per cent over the full range of inertia axis variation considered.

3.2.2. *Flutter Speed as a Function of Taper Ratio.*—The values of flutter speed against taper ratio are plotted in Fig. 13 ($\beta = 0$ deg). These values are the experimental values corrected for wing stiffness and stiffness ratio as described in Part I, section 1.5.2. A comparison of the experimental points with the criterion variation of V proportional to $(1 - 0.8k + 0.4k^2)$ shows reasonable agreement but in fact the experimental variation is approximately linear. Better average agreement with the experimental points is obtained from the curve of V proportional to $(0.9 - 0.33k)$ which gives a maximum deviation of about 10 per cent over the range of taper ratios considered.

3.3. *Criterion for the Swept Wing.*—The effects of inertia axis location and wing taper ratio are similar to those for the unswept wings. In general the experimental variation of flutter speed with inertia axis variation is within 10 per cent of the variation suggested by the criterion and the experimental variation of flutter speed with wing taper is within similar limits of the curve of V proportional to $(0.9 - 0.33k)$, though the criterion variation of V proportional to $(1 - 0.8k + 0.4k^2)$ is more seriously in error.

3.3.1. *Flutter Speed as a Function of Angle of Sweepback.*—The results of critical flutter speed against wing sweepback are plotted for the four wings in Figs. 9 and 10. The values of flutter speed for each wing have been plotted to a reduced scale to give a unit flutter speed parameter at 20 deg sweepback (the minimum sweepback for the modified wings) in Fig. 16. An arbitrary curve of the form V proportional to $\sec^{3/2}(\beta - \pi/16)$ has been drawn passing through the common point at 20 deg sweepback and is in good average agreement with the experimental points for all the wings. For the wing of taper ratio 1 : 2 the values obtained in the theoretical investigation of Part II are also plotted as intermediate points at 5 deg, 15 deg, 25 deg and 45 deg respectively and fit the curve reasonably accurately.

3.4. *Summary of Results for Variation of Flutter Speed with Main Parameters.*—(a) The experimental variation of flutter speed with inertia axis position is in reasonable agreement with criterion variation of V inversely proportional to $(g - 0.1)$.

(b) A variation of flutter speed with taper ratio of the form V proportional to $(0.9 - 0.33k)$ gives better average agreement with the experimental points than the criterion variation of V proportional to $(1 - 0.8k + 0.4k^2)$.

(c) The curve of V proportional to $\sec^{3/2}(\beta - \pi/16)$ is a fair approximation to the form of variation of flutter speed with sweepback for these wings.

3.5. *Proposed Modification to Criterion.*—The above results suggest a modified version of the criterion of R. & M. 2154. Sweepback variation can be incorporated into the original criterion to give

$$\frac{1}{V} \left(\frac{m_0}{\rho_0 \bar{d} c_m^2} \right)^{1/2} = 0.93 \frac{(g - 0.1)(1.3 - h)}{(1 - 0.8k + 0.4k^2)(1 - 0.1r) \sec^{3/2}(\beta - \pi/16)} \quad \dots \quad (2)$$

and finally the criterion can be modified to include the suggested linear variation of flutter speed with taper ratio to give

$$\frac{1}{V} \left(\frac{m_0}{\rho_0 \bar{d} c_m^2} \right)^{1/2} = 0.9 \frac{(g - 0.1)(1.3 - h)}{(0.9 - 0.33k)(1 - 0.1r) \sec^{3/2}(\beta - \pi/16)} \cdot \quad \dots \quad (3)$$

The values of V for all four wings as determined from equations (2) and (3) are given together with the experimental values in Table 4. The results show that equation (3) gives better average agreement with the experimental values than equation (2) over the complete range of sweepback considered. Moreover, equation (3) possesses a certain advantage over equation (2) when considered as a design criterion, for it affords greater relief to the designer for wings in the medium taper (3 : 4 to 1 : 2) region, *e.g.*, for a wing of taper ratio 1 : 2 the flutter speed from equation (3) is 8 per cent higher than that obtained from equation (2), which represents a torsional stiffness margin of 16 per cent.

The introduction of the sweepback function, $\sec^{3/2}(\beta - \pi/16)$, enables the swept-back wing to be treated as the equivalent unswept wing rotated about the root, and the values of m_0 , r and other terms are determined as if the wing were unswept.

3.6. *Further Developments.*—The above proposed amendments to the criterion are only applicable to 'fixed-root' flutter and are based on results for only four wings. Further experimental or theoretical verification is required for their acceptance and investigations⁶, are in fact now in progress which should provide data on this point. The researches in hand or planned will need to be considered to suggest further amendments or alternative approaches to cover the important case of 'body-freedom' flutter.

Acknowledgement.—Acknowledgements are due to Mr. P. J. Cutt of Structures Department, Royal Aircraft Establishment for assistance given in the experimental and analytical work.

TABLE 4

A Comparison of Experimental and Criterion Values of Flutter Speed

Criterion of R. & M. 2154 modified for sweepback

$$V = \left(\frac{m_0}{\rho_0 \bar{d} c_m^2} \right)^{1/2} \frac{(1 - 0.8k + 0.4k^2)(1 - 0.1r)}{0.93(g - 0.1)(1.3 - h)} \sec^{3/2} \left(\beta - \frac{\pi}{16} \right). \quad \dots \quad (A)$$

Proposed new criterion

$$V = \left(\frac{m_0}{\rho_0 \bar{d} c_m^2} \right)^{1/2} \frac{(0.9 - 0.33k)(1 - 0.1r)}{0.9(g - 0.1)(1.3 - h)} \sec^{3/2} \left(\beta - \frac{\pi}{16} \right). \quad \dots \quad (B)$$

Taper ratio	Inertia axis	Flutter speed Sweepback $\beta = 0$ deg			Flutter speed Sweepback $\beta = 20$ deg			Flutter speed Sweepback $\beta = 35$ deg			Flutter speed Sweepback $\beta = 50$ deg		
		<i>k</i>	<i>g</i>	Expt.	<i>A</i>	<i>B</i>	Expt.	<i>A</i>	<i>B</i>	Expt.	<i>A</i>	<i>B</i>	Expt.
1.00	0.40	121	118	117	120	117	116	134	131	128	171	166	155
	0.45	103	101	103	102	100	103	114	112	116	145	142	143
	0.50	90	89	91	89	88	86	100	99	99	127	125	126
0.75	0.40	97	104	102	96	103	104	107	115	116	136	146	142
	0.45	83	89	92	82	88	98	92	99	112	117	125	139
	0.50	73	78	78	72	77	82	81	86	96	103	110	120
0.50	0.40	109	118	121	108	117	122	121	131	139	154	166	168
	0.45	94	101	110	93	100	108	104	112	126	132	142	156
	0.50	82	89	94	81	88	95	91	99	109	116	125	139
0.25	0.40	117	119	127	116	118	126	130	132	142	165	168	183
	0.45	100	102	105	99	101	108	111	113	122	141	144	156
	0.50	88	90	85	87	89	92	97	100	104	123	127	137

REFERENCES

No.	Author	Title, etc.
1	N. C. Lambourne	An Experimental Investigation on the Flutter Characteristics of a Model Flying Wing. R. & M. 2626. April, 1947.
2	E. G. Broadbent	Flutter Problems of High Speed Aircraft. R.A.E. Report Structures 37. A.R.C. 12,398. April, 1949.
3	A. R. Collar, E. G. Broadbent, and E. B. Puttick.	An Elaboration of the Criterion for Wing Torsional Stiffness. R. & M. 2154. January, 1946. Also published by I.C.A.O.
4	F. Smith	Note on the Use of Flight Models for Investigation of Flutter. A.R.C. 11,404. March, 1948. (Unpublished.)
5	H. Glauert	<i>Aerofoil and Airscrew Theory</i> . Chap. XI. Cambridge University Press.
6	H. Templeton	Application of Wing Stiffness Criteria to Swept-back Wings. A.R.C. 11,489. May, 1948. (Unpublished.)

NOTATION

V	Critical flutter speed
s	Wing semi-span from root to tip as measured along the wing flexural axis
c_m	Wing mean chord
d	Wing span to equivalent tip ($= 0.9s$)
g	Position of inertia axis aft of leading edge as fraction of chord
h	Position of flexural axis aft of leading edge as fraction of chord
k	Wing taper ratio ($= \frac{\text{Tip chord}}{\text{Root chord}}$)
k_G	Radius of gyration of wing section about inertia axis as fraction of chord
l_ϕ	Wing flexural stiffness, measured at $0.7s$
m_0	Wing torsional stiffness measured at $0.7s$
n	Frequency of normal wing mode
r	Stiffness ratio ($= \frac{l_\phi}{d^3} / \frac{m_0}{dc_m^2}$)
β	Angle of sweepback of wing flexural axis
ρ_0	Air density at sea level
σc^2	Wing density per unit span

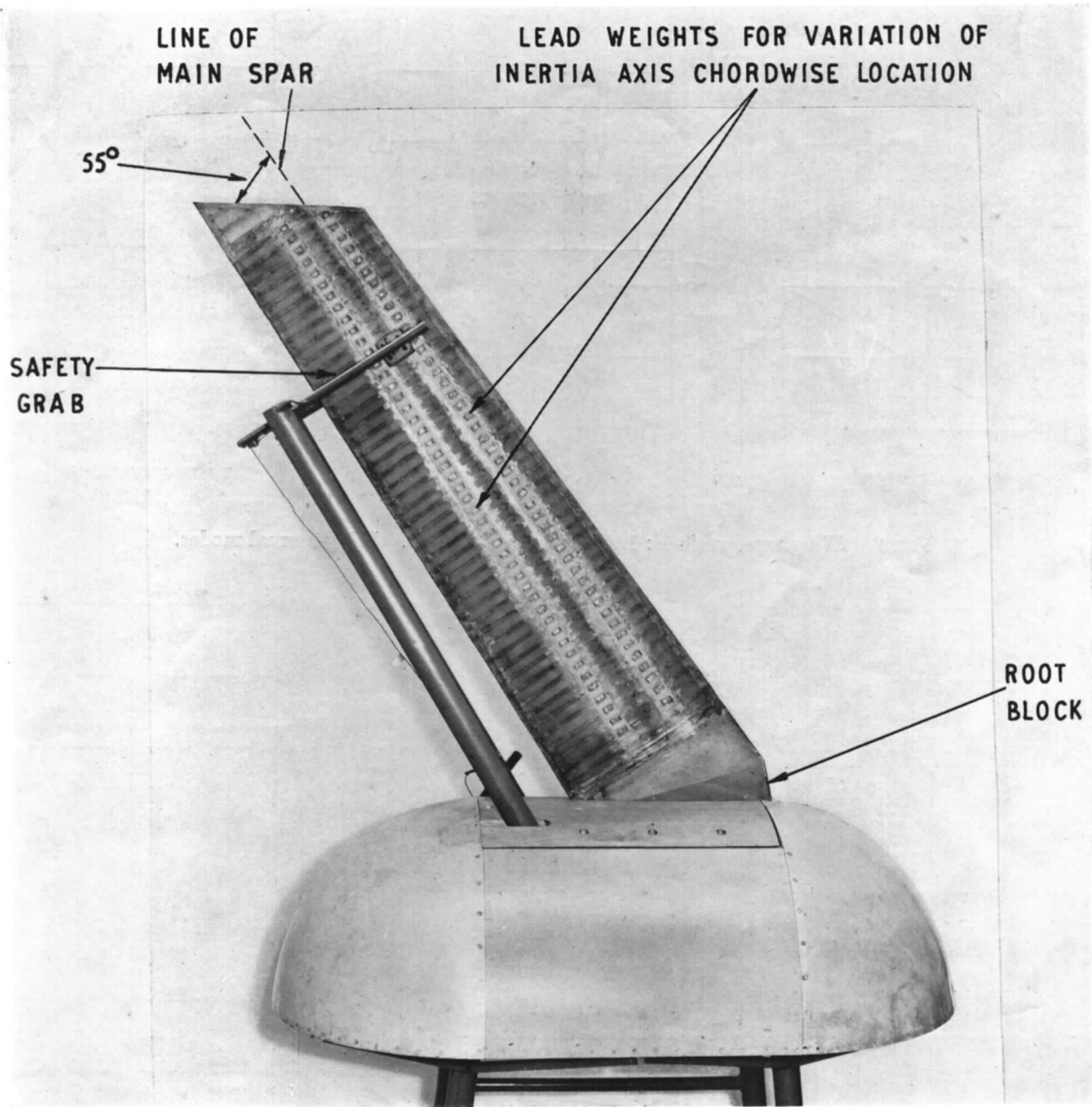


FIG. 1. Model wing and flutter rig.

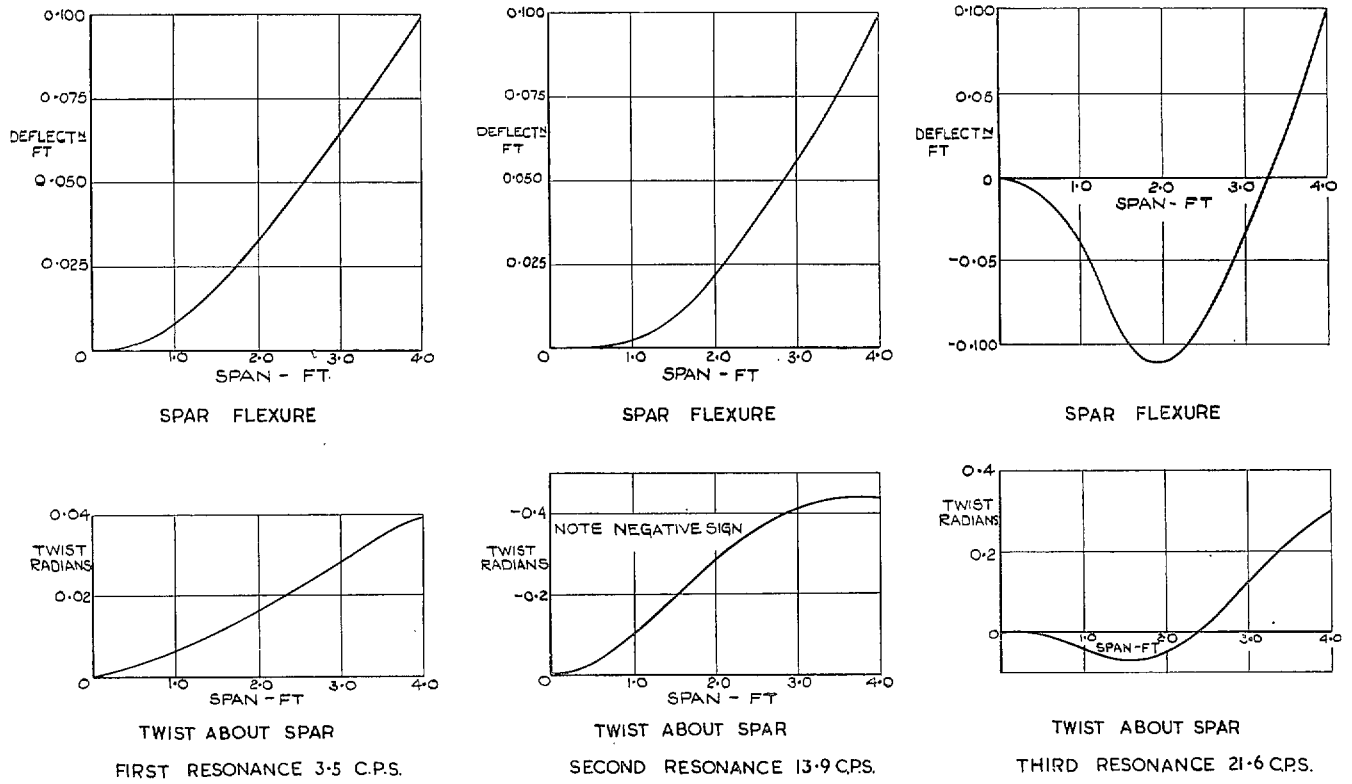


FIG. 2. Wing taper ratio 1 : 1. Inertia axis at $0.5c$. Wing-normal modes.

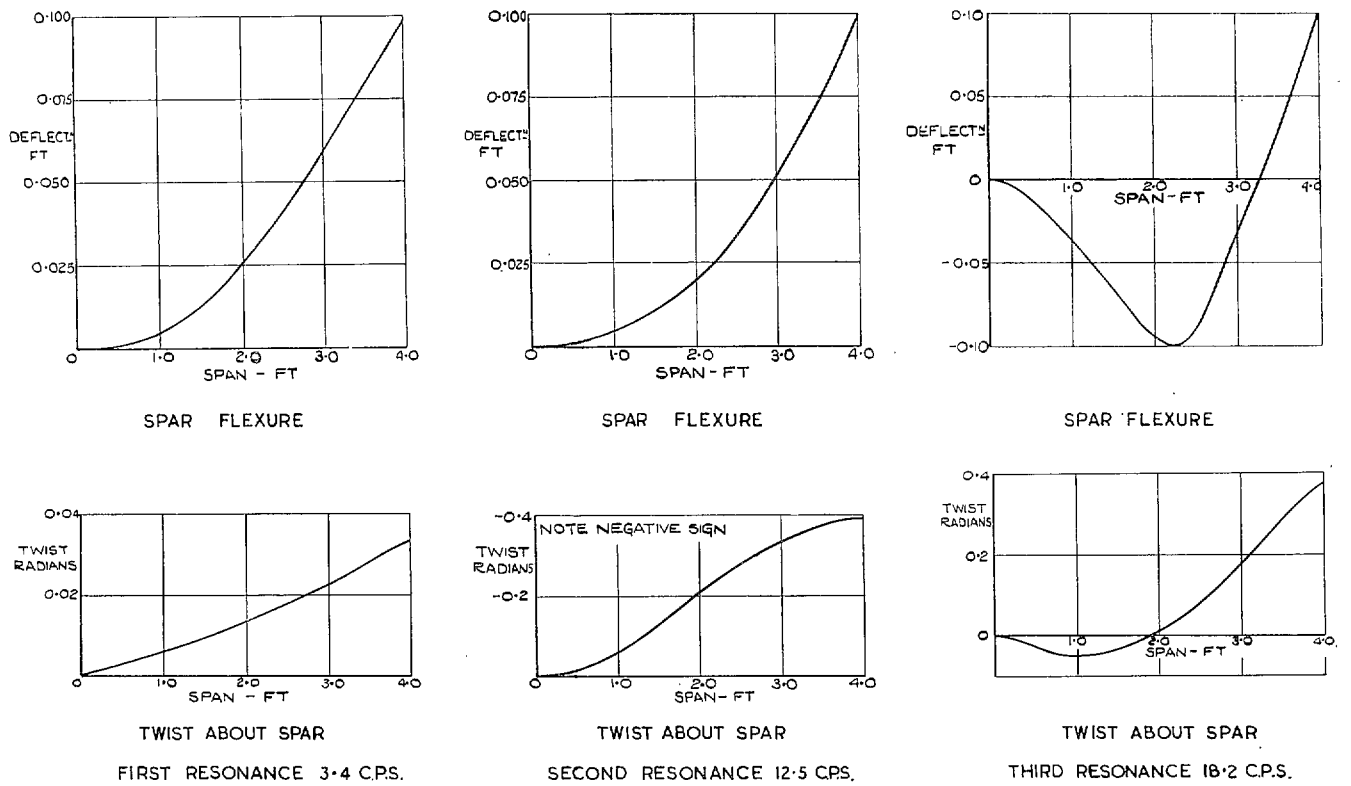


FIG. 3. Wing taper ratio 3 : 4. Inertia axis at $0.5c$. Wing-normal modes.

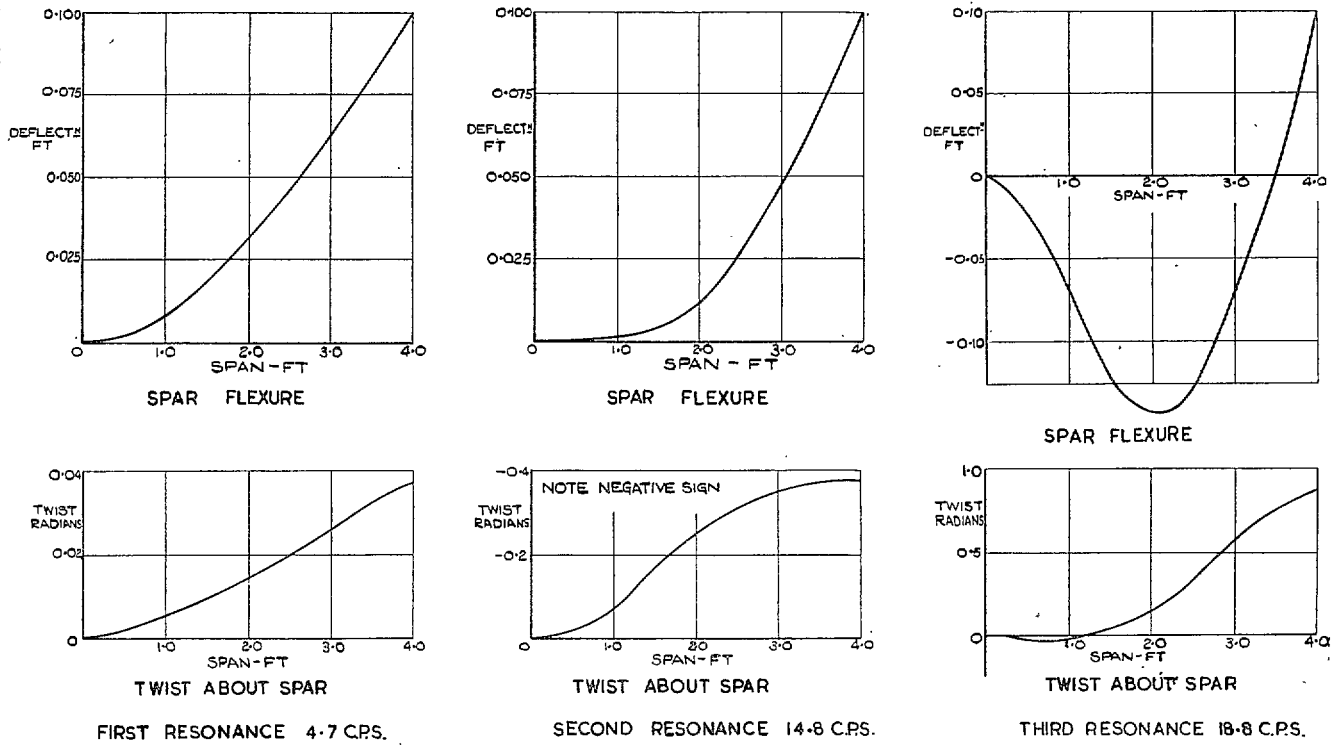


FIG. 4. Wing taper ratio 1 : 2. Inertia axis at $0.5c$. Wing-normal modes.

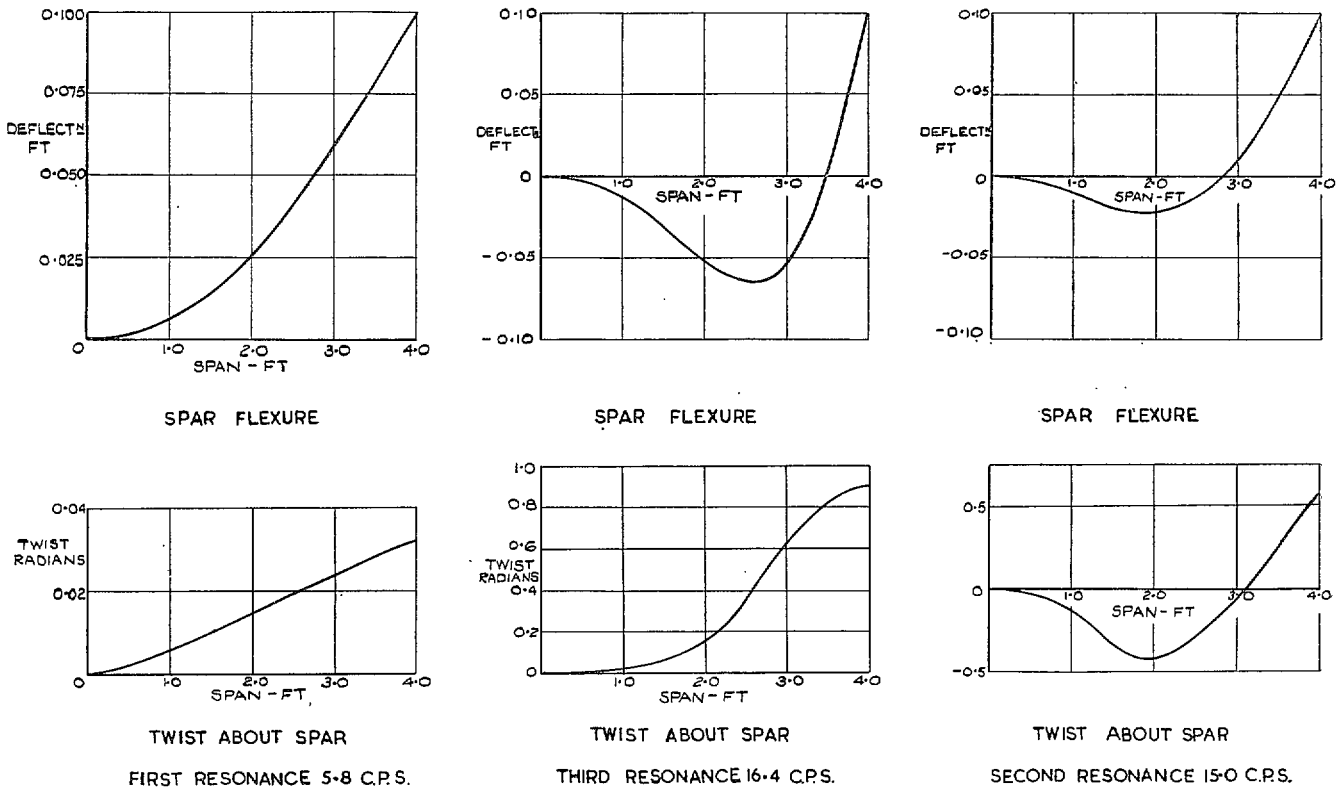


FIG. 5. Wing taper ratio 1 : 4. Inertia axis at $0.5c$. Wing-normal modes.

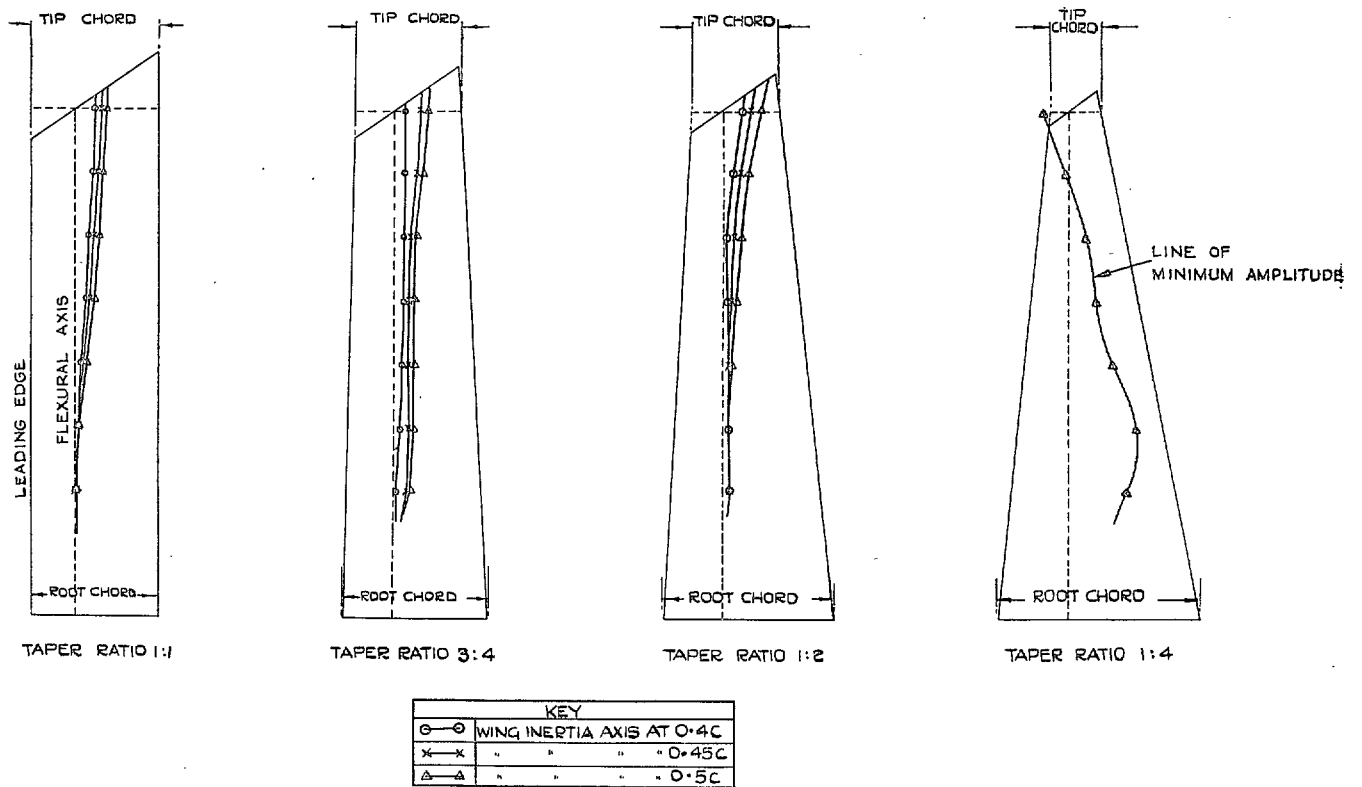


FIG. 6. Variation of wing nodal line location with inertia axis position. Torsion mode.

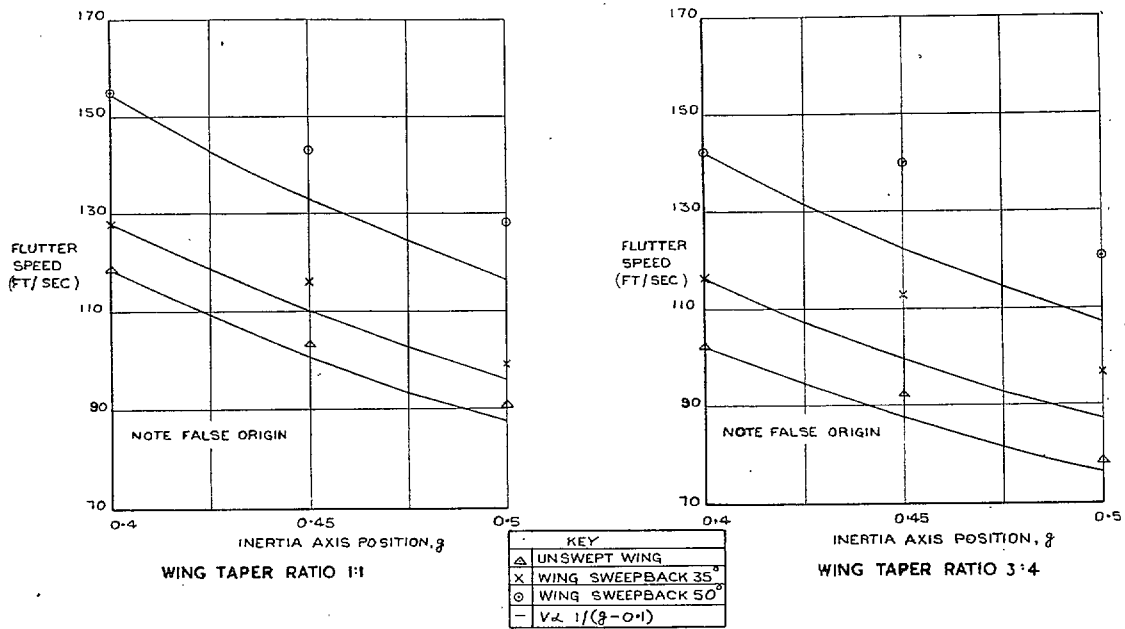


FIG. 7. Variation of flutter speed with inertia axis position at various angles of sweepback.

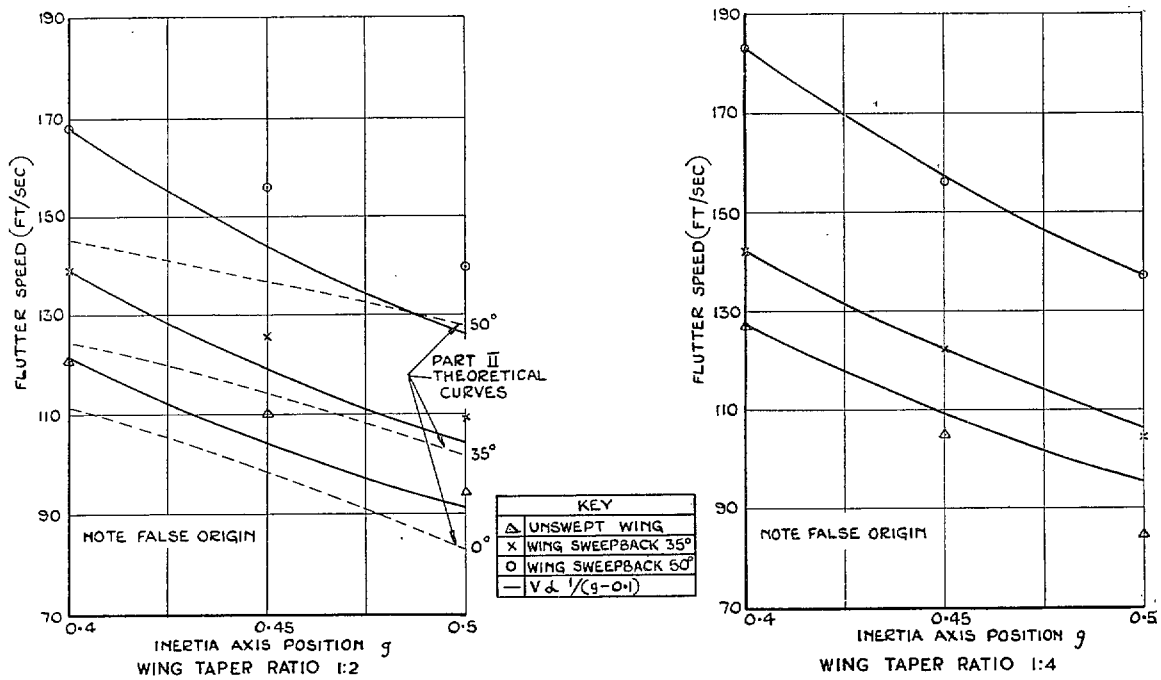
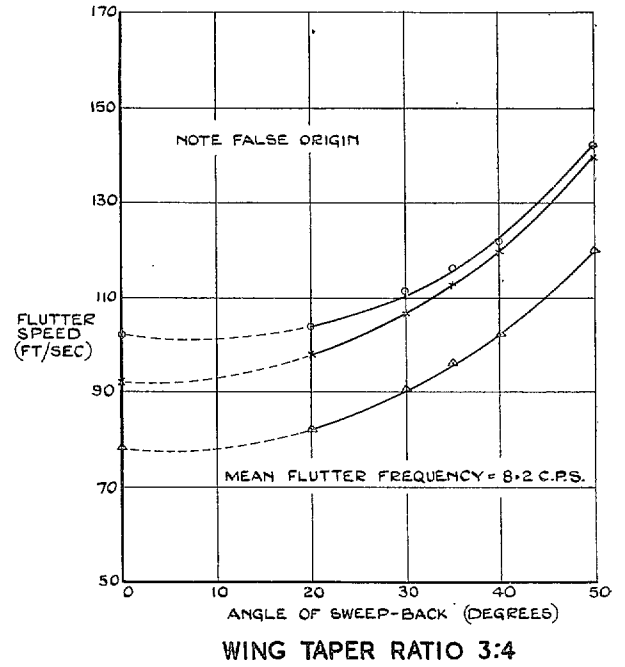
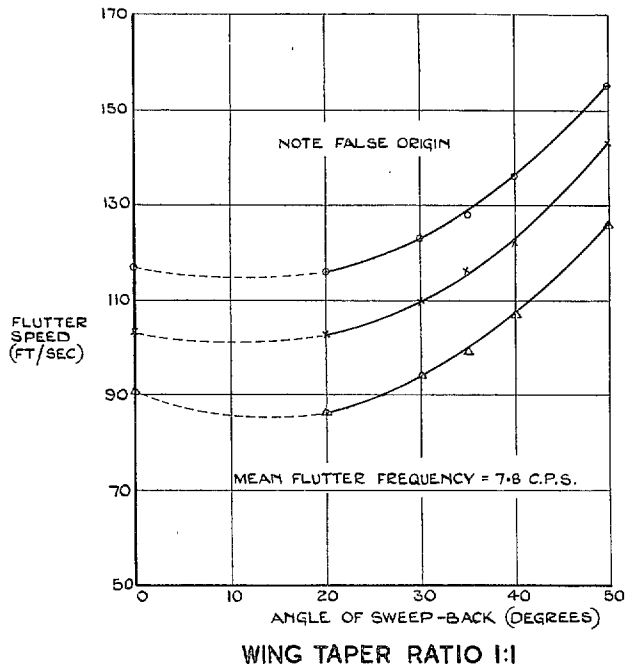
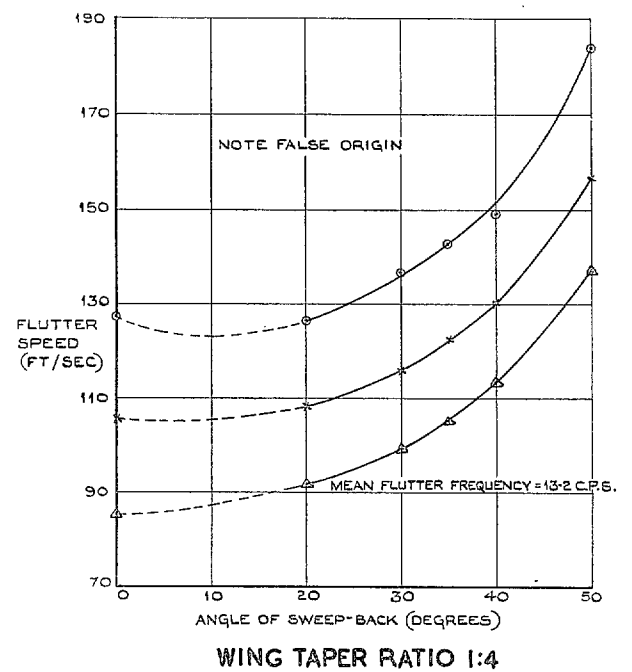
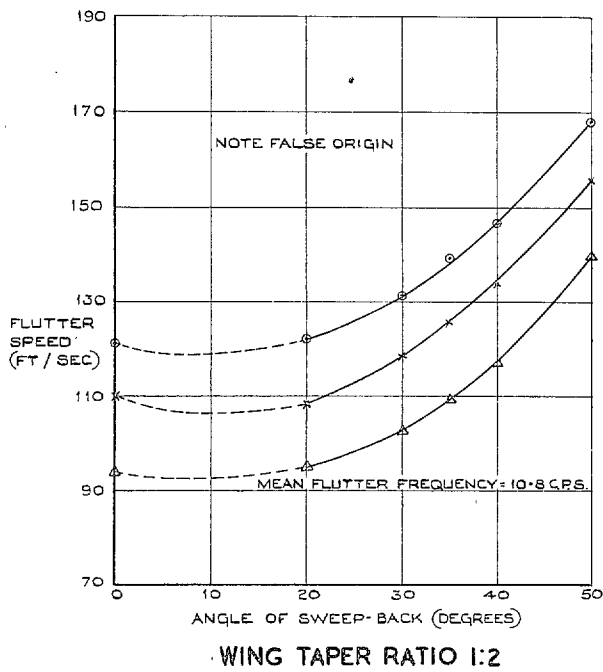


FIG. 8. Variation of flutter speed with inertia axis position at various angles of sweepback.



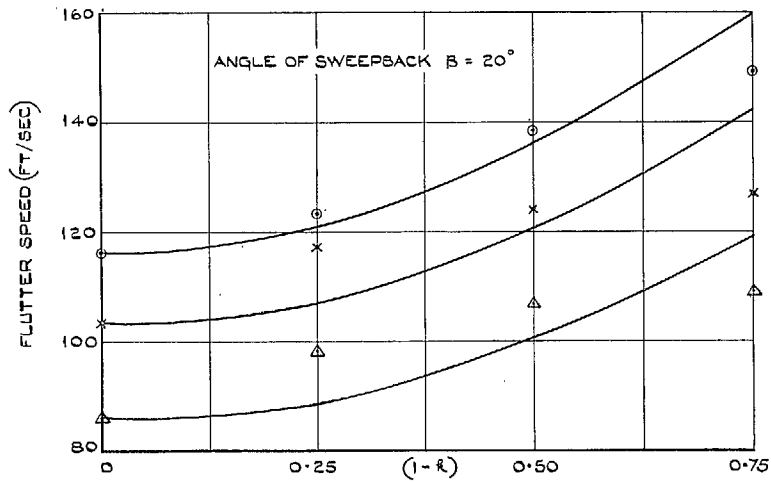
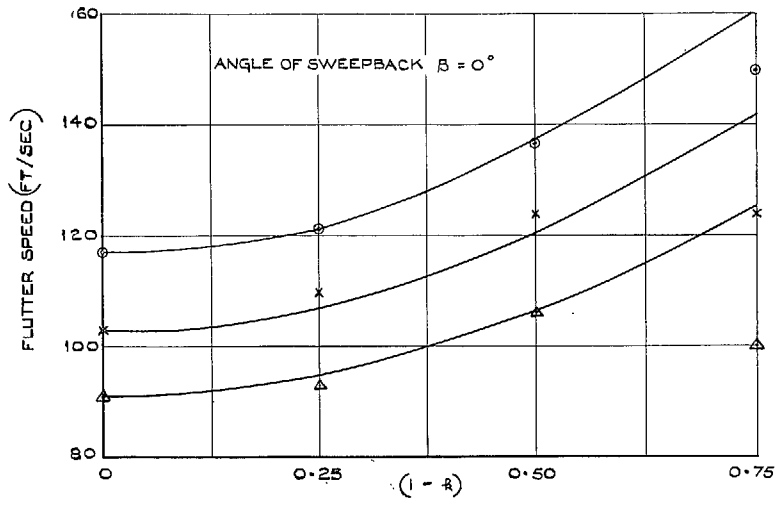
KEY	
○—○	WING INERTIA AXIS AT 0.4C
×—×	" " " " 0.45C
△—△	" " " " 0.5C

FIG. 9. Variation of flutter speed with angle of sweepback at various inertia axis positions.



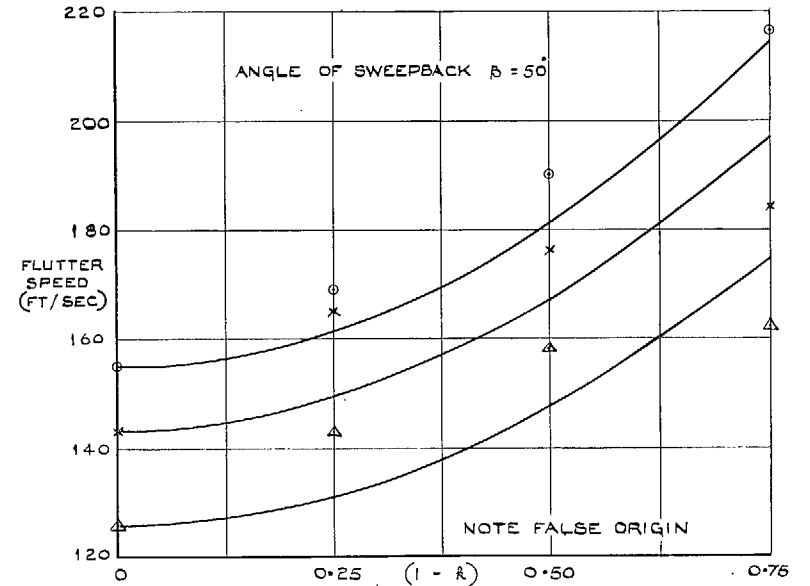
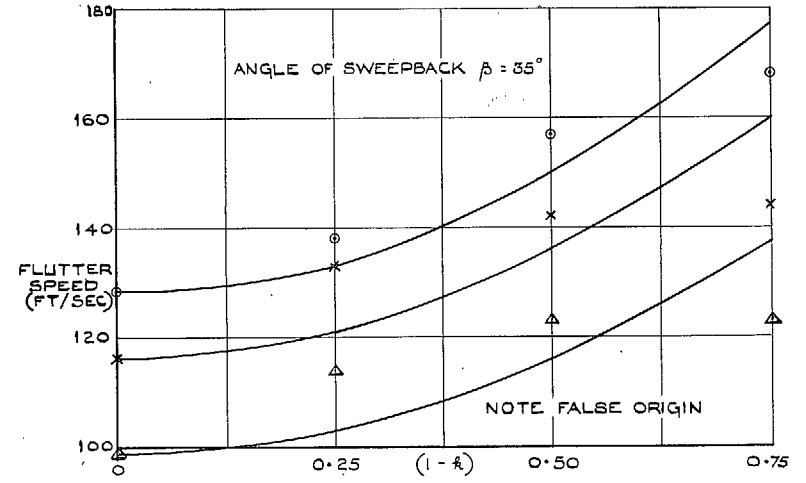
KEY	
○—○	WING INERTIA AXIS AT 0.4C
×—×	" " " " 0.45C
△—△	" " " " 0.5C

FIG. 10. Variation of flutter speed with angle of sweepback at various inertia axis positions.



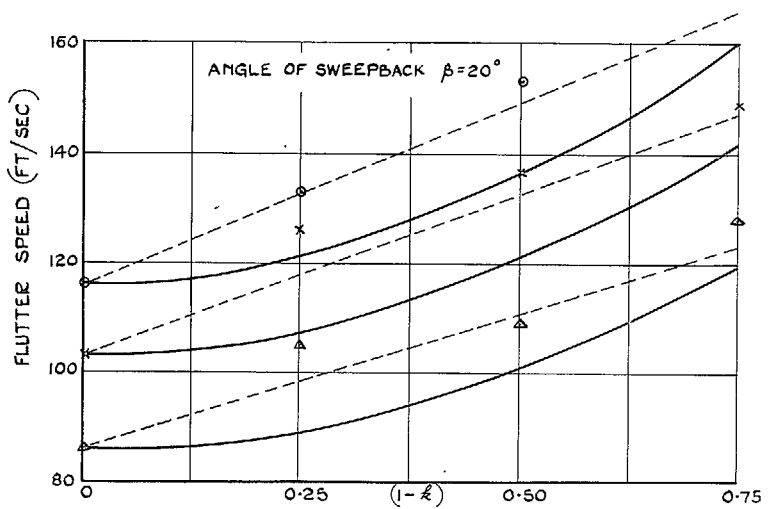
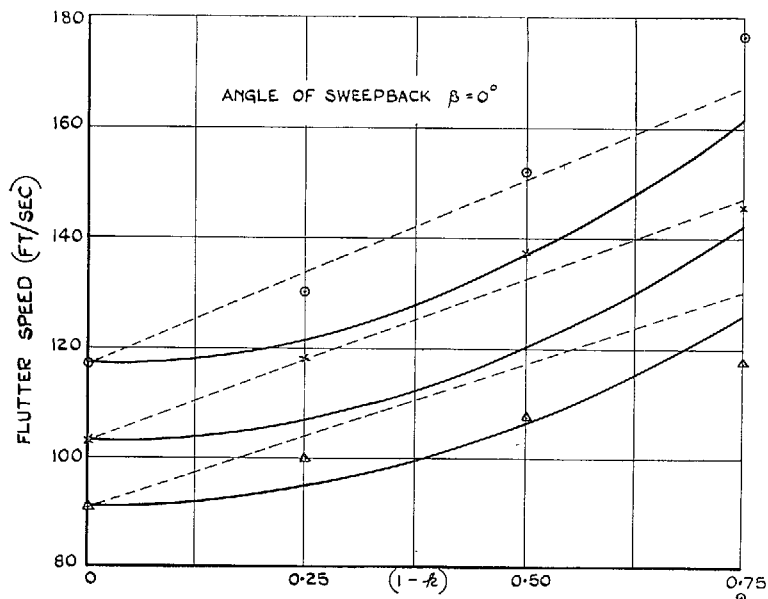
KEY	
○	INERTIA AXIS AT 0.4 C
x	INERTIA AXIS AT 0.45 C
△	INERTIA AXIS AT 0.5 C
—	$V \propto (1 - 0.8r + 0.4r^2)$

FIG. 11. Variation of flutter speed with taper ratio at various inertia axis positions assuming V varies as $m_0^{1/2}$.



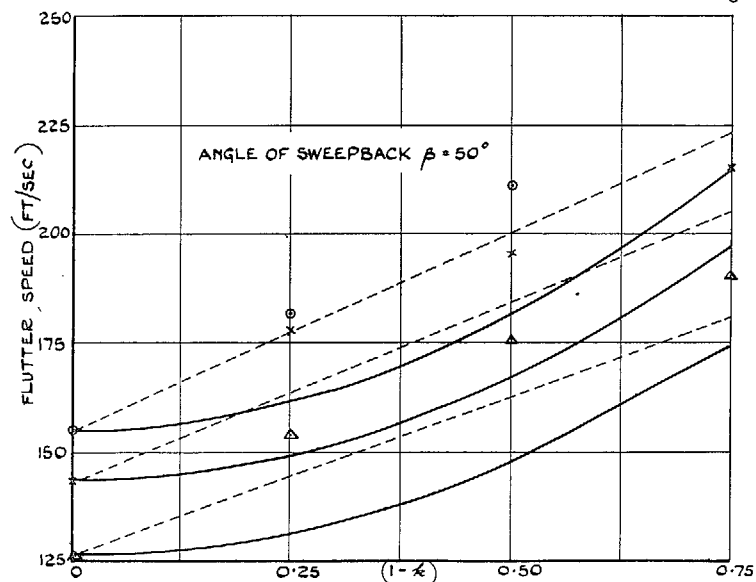
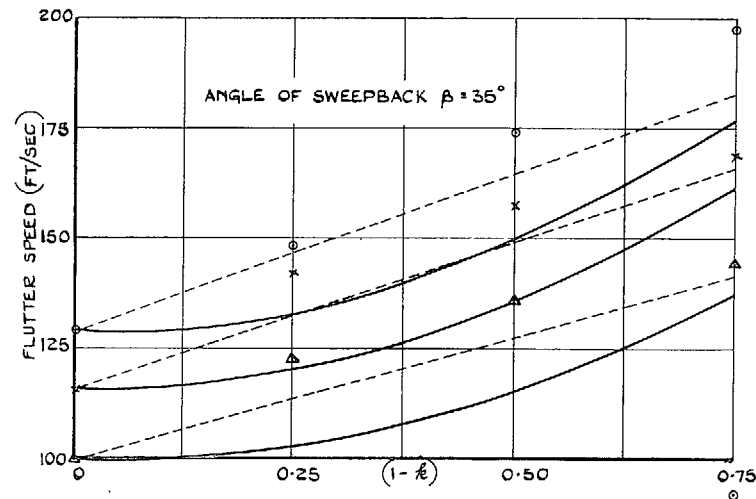
KEY	
○	INERTIA AXIS AT 0.4 C
x	INERTIA AXIS AT 0.45 C
△	INERTIA AXIS AT 0.5 C
—	$V \propto (1 - 0.8r + 0.4r^2)$

FIG. 12. Variation of flutter speed with taper ratio at various inertia axis positions assuming V varies as $m_0^{1/2}$.



KEY	
○	INERTIA AXIS AT 0.4C — $V\alpha c (1 - 0.8k + 0.4k^2)$
x	INERTIA AXIS AT 0.45C --- $V\alpha c (0.9 - 0.33k)$
△	INERTIA AXIS AT 0.5C

FIG. 13. Variation of flutter speed with taper ratio at various inertia axis positions assuming V varies as $m_0^{1/2} (1 - 0.1r)$.



KEY	
○	INERTIA AXIS AT 0.4C — $V\alpha c (1 - 0.8k + 0.4k^2)$
x	INERTIA AXIS AT 0.45C --- $V\alpha c (0.9 - 0.33k)$
△	INERTIA AXIS AT 0.5C

FIG. 14. Variation of flutter speed with taper ratio at various inertia axis positions assuming V varies as $m_0^{1/2} (1 - 0.1r)$.

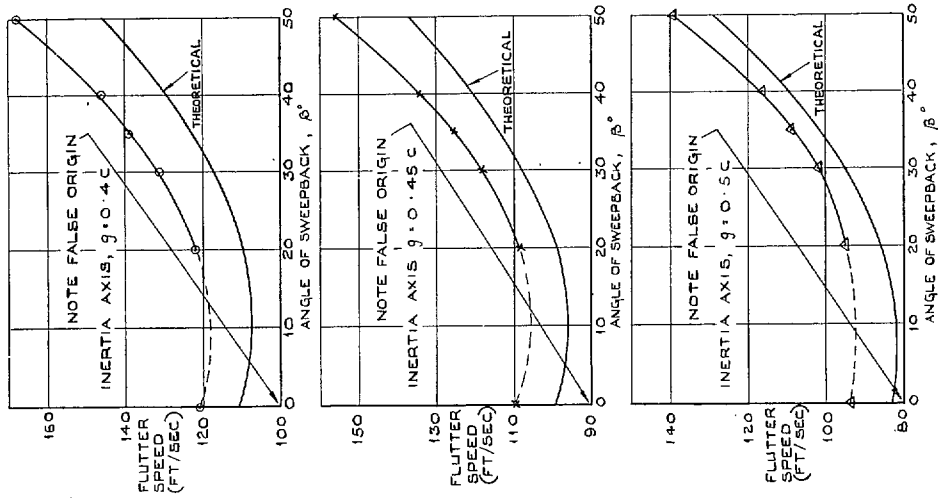
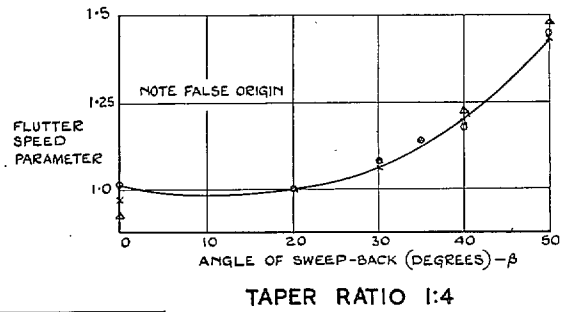
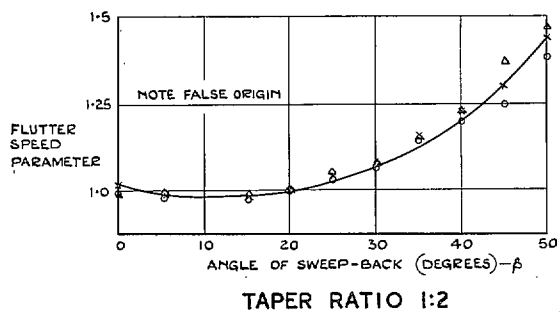
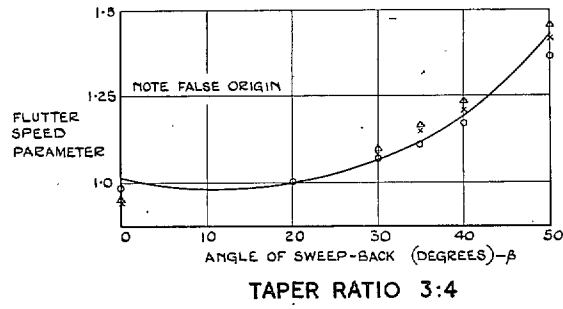
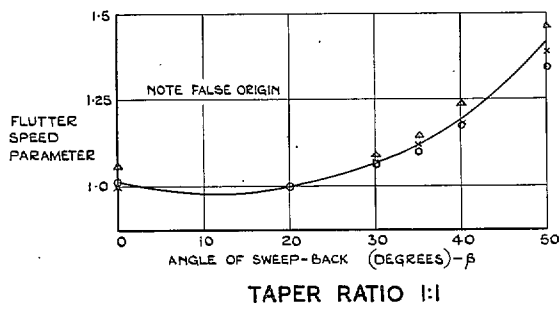


Fig. 15. A comparison of experimental and theoretical results for the wing of taper ratio 1 : 2.



KEY	
○	INERTIA AXIS AT 0.4c
×	INERTIA AXIS AT 0.45c
△	INERTIA AXIS AT 0.5c
—	APPROXIMATION, $V \propto \sec^{3/2}(\beta - \pi/16)$

Fig. 16. Variation of flutter speed with sweepback compared with the function $V \propto \sec^{3/2}(\beta - \pi/16)$.

Publications of the Aeronautical Research Council

ANNUAL TECHNICAL REPORTS OF THE AERONAUTICAL RESEARCH COUNCIL (BOUND VOLUMES)

- 1936 Vol. I. Aerodynamics General, Performance, Airscrews, Flutter and Spinning. 40s. (40s. 9d.)
Vol. II. Stability and Control, Structures, Seaplanes, Engines, etc. 50s. (50s. 10d.)
- 1937 Vol. I. Aerodynamics General, Performance, Airscrews, Flutter and Spinning. 40s. (40s. 10d.)
Vol. II. Stability and Control, Structures, Seaplanes, Engines, etc. 60s. (61s.)
- 1938 Vol. I. Aerodynamics General, Performance, Airscrews. 50s. (51s.)
Vol. II. Stability and Control, Flutter, Structures, Seaplanes, Wind Tunnels, Materials. 30s. (30s. 9d.)
- 1939 Vol. I. Aerodynamics General, Performance, Airscrews, Engines. 50s. (50s. 11d.)
Vol. II. Stability and Control, Flutter and Vibration, Instruments, Structures, Seaplanes, etc. 63s. (64s. 2d.)
- 1940 Aero and Hydrodynamics, Aerofoils, Airscrews, Engines, Flutter, Icing, Stability and Control, Structures, and a miscellaneous section. 50s. (51s.)
- 1941 Aero and Hydrodynamics, Aerofoils, Airscrews, Engines, Flutter, Stability and Control, Structures. 63s. (64s. 2d.)
- 1942 Vol. I. Aero and Hydrodynamics, Aerofoils, Airscrews, Engines. 75s. (76s. 3d.)
Vol. II. Noise, Parachutes, Stability and Control, Structures, Vibration, Wind Tunnels 47s. 6d. (48s. 5d.)
- 1943 Vol. I. (*In the press.*)
Vol. II. (*In the press.*)

ANNUAL REPORTS OF THE AERONAUTICAL RESEARCH COUNCIL—

1933-34	1s. 6d. (1s. 8d.)	1937	2s. (2s. 2d.)
1934-35	1s. 6d. (1s. 8d.)	1938	1s. 6d. (1s. 8d.)
April 1, 1935 to Dec. 31, 1936.	4s. (4s. 4d.)	1939-48	3s. (3s. 2d.)

INDEX TO ALL REPORTS AND MEMORANDA PUBLISHED IN THE ANNUAL TECHNICAL REPORTS, AND SEPARATELY—

April, 1950 - - - - R. & M. No. 2600. 2s. 6d. (2s. 7½d.)

AUTHOR INDEX TO ALL REPORTS AND MEMORANDA OF THE AERONAUTICAL RESEARCH COUNCIL—

1909-1949. R. & M. No. 2570. 15s. (15s. 3d.)

INDEXES TO THE TECHNICAL REPORTS OF THE AERONAUTICAL RESEARCH COUNCIL—

December 1, 1936 — June 30, 1939.	R. & M. No. 1850.	1s. 3d. (1s. 4½d.)
July 1, 1939 — June 30, 1945.	R. & M. No. 1950.	1s. (1s. 1½d.)
July 1, 1945 — June 30, 1946.	R. & M. No. 2050.	1s. (1s. 1½d.)
July 1, 1946 — December 31, 1946.	R. & M. No. 2150.	1s. 3d. (1s. 4½d.)
January 1, 1947 — June 30, 1947.	R. & M. No. 2250.	1s. 3d. (1s. 4½d.)
July, 1951.	R. & M. No. 2350.	1s. 9d. (1s. 10½d.)

Prices in brackets include postage.

Obtainable from

HER MAJESTY'S STATIONERY OFFICE

York House, Kingsway, London, W.C.2; 423 Oxford Street, London, W.1 (Post Orders:
P.O. Box 569, London, S.E.1); 13a Castle Street, Edinburgh 2; 39, King Street, Manchester, 2;
2 Edmund Street, Birmingham 3; 1 St. Andrew's Crescent, Cardiff; Tower Lane, Bristol 1;
80 Chichester Street, Belfast, or through any bookseller

S.O. Code No. 23-2796